

Available online at [www.sciencedirect.com](http://www.sciencedirect.com)**ScienceDirect**

Physics Procedia 50 (2013) 375 – 382

Physics

**Procedia**

International Federation for Heat Treatment and Surface Engineering 20th Congress  
Beijing, China, 23-25 October 2012

## Prediction of Simulating and Experiments for Co-based Alloy Laser Cladding by HPDL

Shirui GUO<sup>a,b</sup>, Zhijun CHEN<sup>a,b</sup>, Dingbao CAI<sup>a,b</sup>, Qunli ZHANG<sup>a,b</sup>, Volodymyr KOVALENKO<sup>c</sup>, Jianhua YAO<sup>a,b,—</sup>

<sup>a</sup>Key Laboratory of E&M (Zhejiang University of Technology), Ministry of Education & Zhejiang Province Hangzhou, 310014, China

<sup>b</sup>Research Center of Laser Processing Technology and Engineering, Zhejiang University of Technology, Hangzhou, 310014, China

<sup>c</sup>Laser Technology Research Institute, National Technical University of Ukraine, Kyiv, 03056, Ukraine

---

### Abstract

In order to investigate the effects of process parameters on the quality of laser cladding layer, Co-based alloy laser cladding experiments based on orthogonal method was performed on the 304 stainless steel by high power diode laser (HPDL). The results show that the laser scanning speed has the most significant influence on the width, height and depth of laser cladding layer, and the powder feeding rate has the most important influence on the hardness of laser cladding layer. For the sake of getting optimum process parameters and reducing the times of process experiments in practical engineering application, a back propagation (BP) neural network model was established to predict the optimum process parameters. The calculation and prediction results show a good agreement with the experimental results. The research results have both significant reference value and guidance meaning in processing parameters of Co-based alloy cladding by a high power diode laser in the application.

© 2013 The Authors. Published by Elsevier B.V. Open access under [CC BY-NC-ND license](https://creativecommons.org/licenses/by-nc-nd/4.0/).

Selection and peer-review under responsibility of the Chinese Heat Treatment Society

*Keywords:* laser cladding; HPDL; Co-based alloy; orthogonal experiment; BP neural network

---

---

\* Corresponding author: Jianhua YAO(1965-), male, professor, Ph.D supervisor, major: laser surface modification. Tel.: +86-571-88320383; fax: +86-571-88320383

*E-mail address:* [laser@zjut.edu.cn](mailto:laser@zjut.edu.cn)

Author: Shirui GUO(1986-), male, Ph.D candidate, major: laser surface modification.

*E-mail address:* [j10312@163.com](mailto:j10312@163.com)

## 1. Introduction

Environmentally friendly manufacturing with laser technology has the advantages of high production efficiency, slight deformation, non-environmental pollution and low dilution rate. In addition, high power diode laser (HPDL) is featured with high converting efficiency, long life span and suitable wavelength, in contrast to the traditional lasers (CO<sub>2</sub>, Nd:YAG). Therefore, it can provide high cost-effectiveness in the industrial application, which means low cost and high production efficiency per unit time. In this study, laser cladding experiments were carried out on the slide valve by using HPDL to improve its wear resistance and prolong its life span.

In order to achieve nice cladding quality, a great amount of exploration experiments were performed to get the appropriate process parameters in actual production. Compared with CO<sub>2</sub> laser, HPDL with the features of high control accuracy, good stability and reliability possesses better process repeatability, which makes the process simulation and parameters prediction of high power diode laser more feasible (Lin Li et al., 2000; Jo Verwimp et al., 2011; Liu JC et al., 2012; Niu ZW et al., 2010). In this paper, Co-based alloy was cladded on the 304 stainless steel by HPDL based on orthogonal experimental design. Then, BP neural network (BP-NN) model was established, based on the research data of orthogonal test. At last, the optimum process parameters were predicted through the BP-NN algorithm, which can guide the practical engineering applications by HPDL.

## 2. Experimental procedure

### 2.1. Experimental condition

The 304 stainless steel was used as the substrate of slide valve. The plate was cut into the samples with size of 55mm×120mm×10mm. Experiments were carried out by high power flexible fiber-coupled diode laser with type of LDF400-2000. Its output wavelength is 900~1030nm and the maximum output power is 2000W. A circular spot with a fixed spot size of 4mm was used in these experiments, and Ar was used to protect laser pool. The cladding powder is the self-fluxing Co-based alloy powder with particle size of 45-105 μm. A self-developed coaxial powder feeding device with a flow closed-loop feedback control was also adopted, and Ar was used as the carrier gas. The feeding rate range is 2~50g/min. The motion device is IRB2400/16 robot with 6 degrees of freedom. After laser cladding, the cladded samples were cut, mosaicked, grinded, polished, etched and dried. The width of the cladding layer (W), height of cladding layer (H), depth of cladding layer (D) and surface microhardness of cladding layer (MH) were measured by a HDX-1000 digital microhardness tester with loading weight of 100g and loading time of 10s.

### 2.2. Experimental design

Three factors and three levels orthogonal experiments were designed to focus on process parameters which have great impacts on the performances of the cladding layer. The three factors include A-laser power (P), B-laser scanning speed (V<sub>s</sub>) and C-powder feeding rate (V<sub>f</sub>). The three levels of P are P<sub>1</sub>=1550W, P<sub>2</sub>=1750W, P<sub>3</sub>=1950W. The three levels of V<sub>s</sub> are V<sub>s1</sub>=360mm/min, V<sub>s2</sub>=540mm/min, V<sub>s3</sub>=720mm/min. The three levels of V<sub>f</sub> are V<sub>f1</sub>=8g/min, V<sub>f2</sub>=13g/min, V<sub>f3</sub>=18g/min. The 9 times L<sub>9</sub> (3<sup>4</sup>) orthogonal experiments were adopted as shown in Table 1. The influences of four indicators, namely: width of cladding layer (W), height of cladding layer (H), depth of cladding layer (D) and surface microhardness of cladding layer (MH) on each factor were investigated. Fig.1 shows the schematic of cross-sectional of the cladding layer, where h is the depth of substrate dilution, D is the total depth of cladding layer, A<sub>1</sub> is the cladding zone, A<sub>2</sub> is the dilution zone, and HAZ is the heat-affected zone. The dilution rate is one of the most important performance indicators. According to geometry definition method of the dilution rate, dilution rate  $\eta = h / (h + H) = h / D$ .

Table 1. Schedule and results of L<sub>9</sub> (3<sup>4</sup>) orthogonal experiments

No.	P/W	V <sub>s</sub> /(mm·min <sup>-1</sup> )	V <sub>f</sub> /(g·min <sup>-1</sup> )	W/mm	H/mm	D/mm	MH/HV <sub>0.1</sub>	η
-----	-----	---	--	------	------	------	----------------------	---

1	1550	360	8	3.483	0.78	1.428	502.46	45.38%
2	1550	540	13	3.114	0.797	0.993	530.32	19.74%
3	1550	720	18	2.621	0.834	0.894	521.30	6.71%
4	1750	540	18	3.582	1.055	1.247	514.40	15.07%
5	1750	720	8	3.311	0.43	0.855	456.54	49.71%
6	1750	360	13	3.976	1.291	1.755	484.94	26.44%
7	1950	720	13	3.045	0.692	1.136	473.12	39.08%
8	1950	360	18	4.197	1.688	1.993	475.60	15.30%
9	1950	540	8	3.316	0.604	1.198	458.30	49.58%

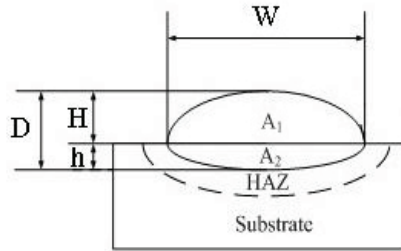


Fig. 1. Schematic of cross-sectional of the laser cladding layer

### 2.3. Results and discussion

Data in Table 1 are used to analyze the effects of different factors and levels on the quality of laser cladding layer. Table 2 shows the effects of different factors A, B, C on each index W, H, D and MH.  $K_{xi}$  represents the total impact of factor i under each level on the index x, for example in Table 2, the first column parameters  $K_{W2}$ , represent the results of factor  $P_2 = 1750W$  under all levels W (as shown in Line 4, 5, 6 in Table 1), namely  $K_{W2} = 3.582 + 3.311 + 3.976 = 10.869$ . Extreme difference  $R_x$  is the difference of the maximum  $K_{xi}$  and the minimum  $K_{xi}$  in the same column, for example in Table 2, the first column,  $R_W = 10.869 - 9.218 = 1.651$ .  $K_{xi}$  means the effect of index x of the cladding layer on the corresponding level of each factor. The higher value shows that the level of the factor has more effect on index x. Extreme difference  $R_x$  represents impact of corresponding factor on index x of the cladding layer in the experiments.

Table 2. Influence of parameters on W, H, D and MH

Index	$K_{xi}$ $R_x$	Factor A	Factor B	Factor C
W	$K_{W1}$	9.218	11.656	10.11
	$K_{W2}$	10.869	10.012	10.135
	$K_{W3}$	10.558	8.977	10.4
	$R_W$	1.651	2.679	0.29
H	$K_{H1}$	2.411	3.759	1.814
	$K_{H2}$	2.776	2.456	2.78
	$K_{H3}$	2.984	1.956	3.577
D	$R_H$	0.573	1.803	1.763
	$K_{D1}$	3.315	5.176	3.481
	$K_{D2}$	3.857	3.438	3.884
	$K_{D3}$	4.327	2.885	4.134

	R <sub>D</sub>	1.012	2.291	0.653
	K <sub>MH1</sub>	1554.08	1463	1417.3
MH	K <sub>MH2</sub>	1455.88	1503.02	1488.38
	K <sub>MH3</sub>	1407.02	1450.96	1511.3
	R <sub>MH</sub>	147.06	52.06	94

From the data in Table 2, the properties of extreme difference  $R_x$  show the degree of impact of each factor on index  $W$ , which is  $V_s > P > V_f$ . Analysis of  $K$  value: the maximum value  $K_{W2}=10.869$  is corresponding to  $P_2$ , the maximum value  $K_{W1}=11.656$  is corresponding to  $V_{s1}$ , and the maximum value  $K_{W3}=10.4$  is corresponding to  $V_{f3}$ . It can be concluded that the cladding layer with the maximum value of  $W$  would be obtained under the experimental conditions of  $P_2=1750W$ ,  $V_{s1}=360\text{mm/min}$ ,  $V_{f3}=18\text{g/min}$ .

According to above analysis, from the rest of Table 2, the impact degree of each factor on index  $H$  is arranged as  $V_s > V_f > P$ ; index  $D$  is arranged as  $V_s > P > V_f$ ; and index  $MH$  is arranged as  $P > V_f > V_s$ . It can be concluded that the maximum value of  $H$  would appear under experimental conditions of  $P_3=1950W$ ,  $V_{s1}=360\text{mm/min}$ ,  $V_{f3}=18\text{g/min}$ ; the maximum value of  $D$  would appear under experimental conditions of  $P_3=1950W$ ,  $V_{s1}=360\text{mm/min}$ ,  $V_{f3}=18\text{g/min}$ ; the maximum value of  $MH$  would appear under experimental conditions of  $P_1=1550W$ ,  $V_{s2}=540\text{mm/min}$ ,  $V_{f3}=18\text{g/min}$ .

### 3. BP-NN model and simulation

Although the experiment data got from the orthogonal experiments are analyzed, it is still difficult to obtain valid prediction and optimization in consideration of the typical non-linear relationship among the complexity of process parameters in laser cladding, the variety of cladding powder materials and the performances. Among all the multilayer feed forward neural network models, BP-NN is the most frequently used one because of better nonlinear mapping capability (Bappa Acherjee et al., 2011 and P. Sathiya et al., 2012). It is widely used in the field of technology of pattern recognition, fault diagnosis, information processing, automatic control and so on (K.R. Balasubramanian et al., 2010; Prasanthi Inakollu et al., 2009; Te-Sheng Li et al., 2010). In order to get more accurate prediction and optimum process parameters for laser cladding, the modified BP-NN model was used as the relationship model between process parameters and performances of the laser cladding layer.

#### 3.1. BP-NN model

It is proved by Kolmogorov theorem that the BP-NN has highly function approximation capability. But it takes more time to train the sample data in order to achieve less error. To improve the convergence rate of the conventional BP-NN, a modified BP-NN model was established by gradient descent algorithms in this paper.

The design structure of BP-NN model is shown in Fig.2. There are three layers: the input layer, hidden layer and output layer, where  $P$ ,  $V_s$  and  $V_f$  three process parameters are set as the output layer,  $W$ ,  $D$ ,  $H$  and  $MH$  four performance parameters are set as the input layer. Taken the Tan-Sigmoid function in Equation (1) as the nonlinear excitation function, the specific configuration parameters of the BP-NN model are shown in Table 3.

$$y = \text{tansig}(x) = \frac{e^x - e^{-x}}{e^x + e^{-x}} \quad (1)$$

Table 3. The configuration parameters of the BP-NN model

Number of neurons in the input layer	4	Learning rate	0.001
Number of neurons in the output layer	3	Momentum factor	0.8
Number of neurons in the hidden layer	9	Maximum epochs	$10^5$
Trans function of hidden layer	tansig	Error goal	$10^{-6}$
Trans function of output layer	purelin	The number of intervals shown	50

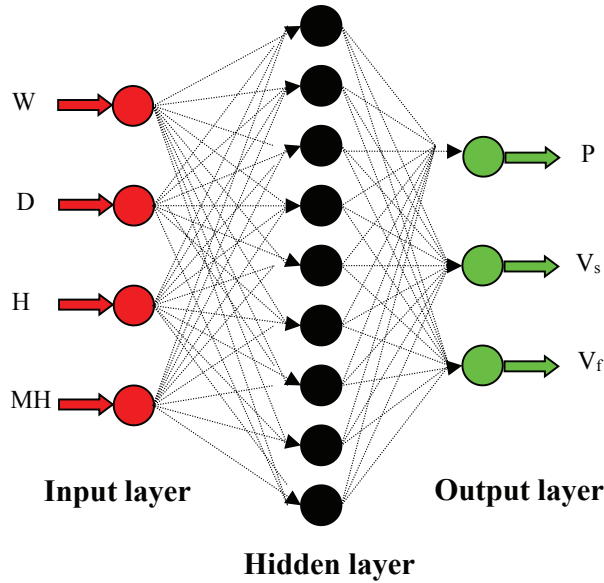


Fig. 2. Structure of BP-NN model for laser cladding Co-based alloy by a HPDL

3.2. Prediction verification based on BP-NN algorithm

The order of magnitude of sample data has a great difference between powder feeding rate and laser power. In order to improve the prediction accuracy of BP-NN model and reduce the relative error of prediction results by the model, the sample data were normalized with Equation (2). All the parameters were normalized to 0.3-1. The output values of BP-NN prediction are converted into the real value with Equation (3). The  $x$ ,  $x_{max}$  and  $x_{min}$  are the original data, the maximum and minimum values of the same parameter respectively, and  $x'$ ,  $x'_a$ ,  $x_a$  are processed data, predicted value and output value of reduction respectively.

$$x' = \frac{7(x - x_{min})}{10(x_{max} - x_{min})} + \frac{3}{10} \tag{2}$$

$$x_a = x_{min} + \frac{1}{7}(10x'_a - 3)(x_{max} - x_{min}) \tag{3}$$

The backward reasoning of process test was used in the experiments to ensure the scientificness of the research method. The key to obtain a good cladding layer is to control the dilution rate, because the dilution rate has direct influence on the properties of cladding layer. The orthogonal experiments show that the rate of dilution of the cladding layer reduces with the increase of the powder feeding rate. In this paper, process verification experiments have been carried out by using the random process parameters in Table 4 when the powder feeding rate is 18g/min. The data of backward reasoning from actual performance parameters and prediction of simulating process parameters are listed in Table 4. The comparison data of experimental results with predicted results and the absolute relative error are shown in Table 4 as well ("\*" is the simulation value).

Table 4. Comparison of experiment results and predicted results

No.P/W	$V_s$ /(mm·min <sup>-1</sup> )	$V_f$ /(g·min <sup>-1</sup> )	W/mm	H/mm	D/mm	MH/HV <sub>0.1</sub>	Average error
1 1950	390	18	3.315	1.467	1.876	457.15	

1*	2022.894	395.965	16.105					5.27%
2	1950	420	18	4.095	1.507	1.812	493.35	
2*	2177.499	444.101	16.798					8.03%
3	1800	390	18	4.039	1.385	1.672	562.35	
3*	1892.957	368.205	16.536					6.29%
4	1550	540	18	3.365	1.068	1.162	544.94	
4*	1756.642	561.119	15.891					9.65%
5	1550	480	18	3.252	1.098	1.221	545.92	
5*	1596.411	421.223	17.537					5.94%

The minimum average relative error is 5.27% in Table 4. The error is smaller than the result from the stability of laser and corresponding equipment in actual production. The results show that BP-NN model plays well in the prediction. Taking into account of the maximum laser power 2000W in the experiment, the value is regarded as 2000W when the prediction value is higher than 2000W.

### 3.3. Simulation of optimum process parameters

In order to achieve the optimum process parameters of Co-based alloy cladding by diode laser easily, the equations in Table 5 are used as the performance indicators evaluation equation. In these equations, the higher value of M, the better performance can achieve.  $W_n$ ,  $D_n$ ,  $H_n$  and  $MH_n$  are normalized data of W, D, H and MH, namely direct output data of BP-NN model. Superior performances of the cladding layer can be obtained when the dilution rate is 0.1, so  $(\eta-0.1)$  is regarded as an evaluation factor of comprehensive performance.

Four typical cases are selected as the evaluation criterions (i.e. W, D, MH and comprehensive performance). Because the functions of backward reasoning and forward reasoning based on the determined configuration parameters of BP-NN model are similar, the optimum process parameters are explored by using backward reasoning of BP-NN model. There are 26896-run mixed experiments used the orthogonal experimental method for the prediction; the parameters are  $P_1=1500W$ ,  $P_2=1510W$ ,.....,  $P_{31}=1900W$ ,  $V_{s1}=300mm/min$ ,  $V_{s2}=310mm/min$ ,.....,  $V_{s31}=700mm/min$ ,  $V_{f1}=5g/min$ ,  $V_{f2}=6g/min$ ,.....,  $V_{f11}=20g/min$ , etc. The main purpose is to find the maximum value of M in four evaluation equations ( $W_{nmax}$ ,  $D_{nmax}$ ,  $MH_{nmax}$  and  $M4_{max}$ ).

Table 5. The coefficients and function of the evaluation equation

Purpose of evaluation equation	Equation
To search for a process parameter of W maximum	$M1=W_n$
To search for a process parameter of D maximum	$M2=D_n$
To search for a process parameter of MH maximum	$M3=MH_n$
To search for an optimum parameter of better comprehensive performance	$M4=W_n^2 D_n^2 MH_n^2 (\eta-0.1)^2$

In order to show projections more intuitively, the dimension of the powder feed rate is removed in the simulation figure. The three-dimensional simulation value (P,  $V_s$ , and M) of  $W_{nmax}$ ,  $D_{nmax}$ ,  $MH_{nmax}$  and  $M4_{max}$  are shown in Fig 3. In consideration of the great influence of dilution rate on the performance of cladding layer, the simulation value data of the dilution rate between 5%~20% is selected to explore optimum parameters. The corresponding parameters of  $M_{max}$  in predicting outcome are shown in Table 6. Array 1, 2, 3 and 4 in Table 6 are width of cladding layer ( $W_n$ ), the depth of cladding layer ( $D_n$ ), microhardness ( $MH_n$ ) and optimum parameters respectively.

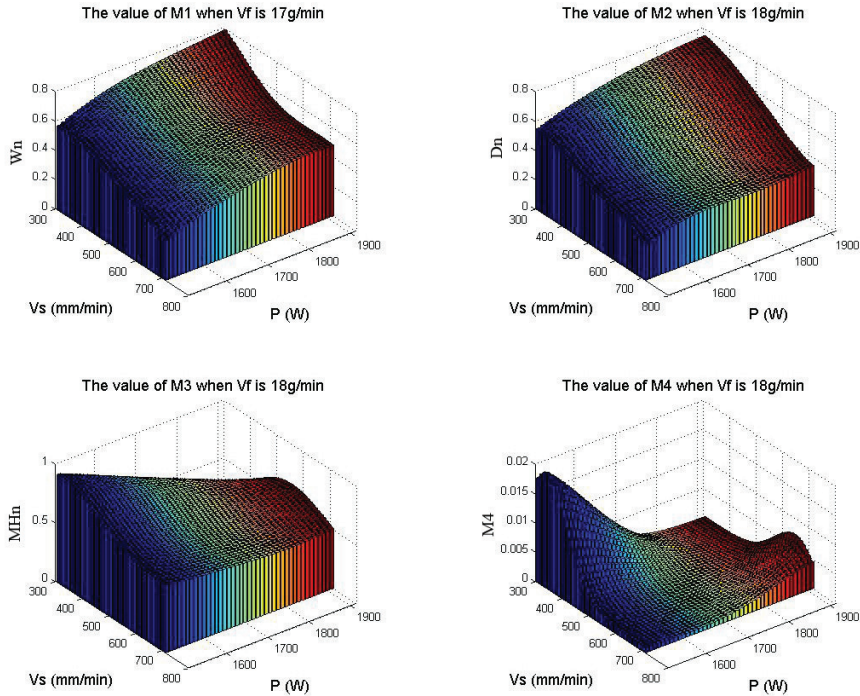


Fig. 3. Predictive value of the maximum M value of the four evaluations

Table 6. The corresponding parameters of four evaluation index  $M_{max}$  value

No.	P/W	$V_s/(mm \cdot min^{-1})$	$V_f/(g \cdot min^{-1})$	W/mm	H/mm	D/mm	MH/HV <sub>0.1</sub>	Average error	$\eta$	M
1	1750	360	17	4.210	1.495	1.821	488.58		17.90%	
1*				4.373	1.544	1.803	508.299	3.05%	14.36%	0.6789
2	1800	360	18	3.901	1.633	1.995	486.56		18.15%	
2*				4.023	1.702	2.042	517.727	4.03%	16.65%	0.6838
3	1550	410	18	3.707	1.129	1.273	585.73		11.31%	
3*				3.312	1.102	1.197	596.199	5.20%	7.94%	0.8290
4	1550	410	18	3.707	1.129	1.273	585.73		11.31%	
4*				3.312	1.102	1.197	596.199	5.20%	7.94%	0.0105

Co-based alloy laser cladding experiments were performed by using the process parameters in Table 6, and the actual results are shown with “\*”. The results of the model test are approximately matching the actual results and the results of previous 14 experimental groups (as shown in Table 1 and Table 4). The optimum parameters of the Co-based alloy cladding experiment are  $P=1550W$ ,  $V_s=410mm/min$ ,  $V_f=18g/min$ , and the dilution rate of cladding layer under the process parameters is 11.31%, which is close to the optimal dilution rate of laser cladding. Hence, the BP-NN model is feasible and effective in practical application, and it also has significant reference value and guidance meaning for process design of Co-based alloy cladding by a high power diode laser in engineering application.

#### 4. Conclusions

(1) Qualitative analysis of the interaction characteristics among various factors can be obtained by the experimental samples based on orthogonal experimental design.

(2) BP-NN model for Co-based alloy cladding by a high power diode laser was established in this paper. The mapping relationship between properties of cladding layer and process parameters can be determined by training the process experiment data.

(3) Prediction and validation of experimental results based on BP-NN algorithm show that the mean absolute relative error between the predictive values and the experimental values is no more than 10%. The method is feasible and effective in the process parameter prediction.

(4) In this study, the optimum parameters for Co-based alloy cladding by a diode laser based on simulation and process experiments is  $P=1550\text{W}$ ,  $V_s=410\text{mm/min}$ ,  $V_f=18\text{g/min}$ . The research results have significant reference value and guidance meaning for process design of Co-based alloy cladding by a high power diode laser in engineering application.

#### Acknowledgements

The authors would like to appreciate financial supports from State International Technology Cooperation Project (KM-JD-2012002), and Zhejiang Provincial Commonweal Technology Application Research International Cooperation Project (2011C24006).

#### References

- Lin Li. The advances and characteristics of high-power diode laser materials processing. *Optics and lasers in engineering*, 2000;34:231-253.
- Jo Verwimp, Marleen Rombouts, Eric Geerinckx, Filip Motmans. Applications of laser clad WC-based wear resistant coatings. *Physics procedia*, 2011;12:330-337.
- Liu JC, Ni LB. Prediction of laser clad parameters based on neural network. *Materials Technology*, 2012;27:11-14.
- Niu ZW, Song K, Li ZY. Quality prediction of laser cladding based on evolutionary neural network. *Advanced Materials Research*, 2010;44-47:2310-2313.
- Bappa Acherjee, Subrata Mondal, Bipan Tudu, Dipten Misra. Application of artificial neural network for predicting weld quality in laser transmission welding of thermoplastics. *Applied Soft Computing*, 2011;11:2548–2555.
- P. Sathiya, K. Panneerselvam, M.Y. Abdul Jaleel. Optimization of laser welding process parameters for super austenitic stainless steel using artificial neural networks and genetic algorithm. *Materials and Design*, 2012;36:490–498.
- K.R. Balasubramanian, G. Buvanashakaran, K. Sankaranarayanan. Modeling of laser beam welding of stainless steel sheet butt joint using neural networks. *CIRP Journal of Manufacturing Science and Technology*, 2010;3:80-84.
- Prasanthi Inakollu, Thomas Philip, Awadhesh K. Rai, Fang-Yu Yueh, Jagdish P. Singh. A comparative study of laser induced breakdown spectroscopy analysis for element concentrations in aluminum alloy using artificial neural networks and calibration methods. *Spectrochimica Acta Part B*, 2009;64:99-104.
- Te-Sheng Li, Chih-Ming Hsu. Parameter optimization of sub-35 nm contact-hole fabrication using particle swarm optimization approach. *Expert Systems with Applications*, 2010;37:878-885.